Proceedings Paper:
Campisano, F, Ozel, S, Ramakrishnan, A et al. (4 more authors) (2017) Towards a Soft Robotic Skin for Autonomous Tissue Palpation. In: IEEE International Conference on Robotics and Automation Systems (ICRA 2017). ICRA 2017, 29 May - 03 Jun 2017, Singapore. IEEE , pp. 6150-6155. ISBN 978-1-5090-4633-1

https://doi.org/10.1109/ICRA.2017.7989729

Towards a Soft Robotic Skin for Autonomous Tissue Palpation

Federico Campisano[1], *Student Member, IEEE*, Selim Ozel[2], *Student Member, IEEE*, Anand Ramakrishnan[2]
Anany Dwivedi[2], Nikolaos Gkotsis[1], Cagdas D. Onal[2], *Member, IEEE*
and Pietro Valdastri[1,3], *Senior Member, IEEE*

***Abstract*— Manual palpation is commonly used to localize tumors and other features buried deep inside organs during open surgery. This approach is not feasible in minimally invasive or robotic surgery, as the contact with the tissue is mediated by instruments. To address this problem, we propose a soft robotic skin (SRS) that can be deployed from a small incision and create a stiffness map in a single step. Such a skin is composed of a matrix of soft robotic tactile elements (SRTEs), each one able to expand and record the tissue response during expansion. In this paper, we firstly prove the feasibility of palpation using a single SRTE. Then, we present and test a soft-suction based anchoring mechanism able to keep the SRS in the desired position in contact with the tissue, allowing surgeons to palpate different sides of the organ. Finally, we detail a calibration method for the SRTE, and assess the feasibility of identifying lumps buried inside a soft tissue phantom, and then inside a chicken liver during an *ex-vivo* trial. Experimental results show that the SRTE was able to differentiate simulated lumps (up to 3.25 mm deep) from healthy tissue in both the phantom and the *ex-vivo* trials. These results, added to the ability of the suction gripper to compensate for the expansion forces of each SRTE, are paving the way for soft robotic autonomous tools that can be used for intraoperative mapping of tissue cancers.**

I. INTRODUCTION

In both laparoscopic and robotic surgery, the surgeon has almost no option to use tactile sensations to define the margins of a tumor, which is typically stiffer than the surrounding healthy tissue. Without this sense of touch, it is often difficult for the surgeon to do a complete resection of a tumor without sacrificing normal tissue, or to explore non-visible organ features by palpation [1].

Tactile mapping would be beneficial for a number of laparoscopic procedures, spanning from partial liver resection (28,720 new hepatic cancer cases and 20,550 deaths in the USA for year 2012 [2]) to radical prostatectomy (2,707,821 cases in 2011 in the USA [2]). While these cancers are commonly removed via open surgery, laparoscopic and robotic approaches have been increasingly adopted [3], [4].

This work was supported by the Royal Society, and by the Vanderbilt Institute for Surgery and Engineering. Any opinions, findings and conclusions, or recommendations expressed in this material are those of the authors and do not necessarily reflect the views of the Royal Society, or VISE.

[1]F. Campisano and N. Gkotsis are with the STORM Lab, Department of Mechanical Engineering, Vanderbilt University, Nashville, TN, USA.federico.campisano.1@vanderbilt.edu

[2]S. Ozel, A. Ramakrishnan, A. Dwivedi, and C. D. Onal are with the WPI Soft Robotics Lab, Department of Mechanical Engineering and Robotics Engineering Program, Worcester Polytechnic Institute, Worcester, MA, USA.

[3]P. Valdastri is with the Department of Robotics and Autonomous System, University of Leeds, Leeds, UK.

F. Campisano and S. Ozel contributed equally to this work.

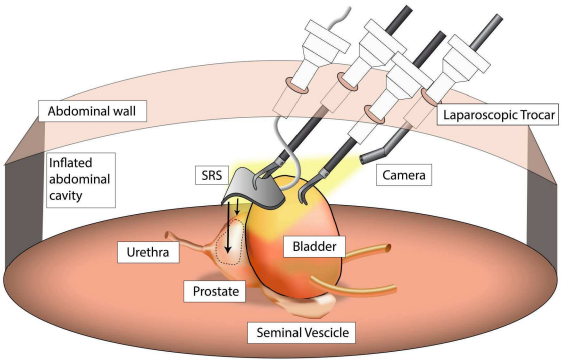

Fig. 1: The soft robotic skin (SRS) introduced into the abdomen through a laparoscopic trocar and deployed on the prostate using laparoscopic forceps.

Intraoperative tactile and kinesthetic sensing in laparoscopic and robotic surgery has been an active research topic for more than two decades [5], [6]. Some of the proposed solutions rely on the surgeon to apply pressure for interrogating the tissue, either directly [7], [8], [9] or via bilateral manipulation [10], [11], [12], [13]. This may result in inconsistent tissue property determination as soft tissue reaction force is non-linearly related to indentation depth. Automated scanning procedures [14], [15] or autonomous tissue exploration [16] may offer more reliable results and facilitate the surgical work-flow, as palpation can proceed without the need for a dedicated surgeon.

Palpation instruments developed to date usually have one sensing unit that indents one spot on the target tissue at a time, following a serial pattern. Therefore, a palpation procedure requires a significant time to complete. Moreover, the tissue may shift as the probe moves from one position to another, leading to inconsistent results. In our approach, we envision a soft robotic skin (SRS) that is inserted from one minimal incision and anchored on top of the target tissue via suction generated by soft grippers (Fig. 1).

The desired SRS is composed of an equispaced matrix of soft robotic tactile elements (SRTEs), each equipped with a pressure sensor facing the tissue and a fluidic chamber that can be expanded by introducing an incompressible liquid (Fig. 2). Suction grippers maintain the SRS in contact with the tissue and compensate for the expansion forces. The use of suction grippers in laparoscopy is not new and has been successfully investigated in the last decade [17], [18], showing reduced skill-dependent damage to the tissues.

The proposed approach would allow the mechanical in-

dentation of an entire surface covered at once, reducing the procedural time and preventing the organ (e.g., prostate in Figs. 1 and 2) from moving during the process. In this scenario, the SRS can effectively play an important role in assisting the surgeon for the correct removal of cancerous tissue during the operation.

This paper focuses on the feasibility of intraoperative palpation using a single SRTE. Firstly, its design and fabrication is presented with the idea of characterizing both the mechanical behaviour and the detection ability (i.e., depth of buried lumps, dimensions). Then, a calibration method is proposed and explained. Finally, the feasibility of identifying lumps buried inside a soft tissue is validated with both a phantom and an *ex-vivo* trial. Intraoperative docking has also been validated by fabricating miniature suction grippers that can compensate for the expansion forces.

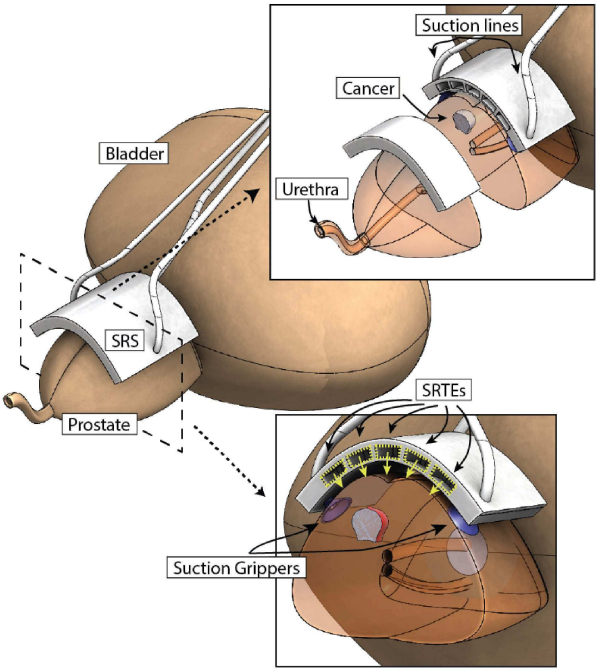

Fig. 2: The SRS docked on the prostate using suction grippers. Each SRTEs can be expanded towards the tissue to obtain a mechanical stiffness map at one time.

II. Soft Robotic Tactile Element

A. Principle of Operation

An individual SRTE has a square shape with a cylindrical hollow chamber in the center as seen in Fig. 3.

Tubing allows the chamber to be filled and expanded with an incompressible fluid (water or saline solution). Two different silicone rubber materials are used in the design. The internal cylindrical surface and the back of the chamber, constrained by a layer of inextensible material, are made out of DragonSkin 30 (Smooth-On USA), while Ecoflex 00-30 (Smooth-On USA) is used for the membrane facing the tissue. The two materials have different elasticity (shore hardness 30A for Dragonskin30 and 00-30 for Ecoflex) and

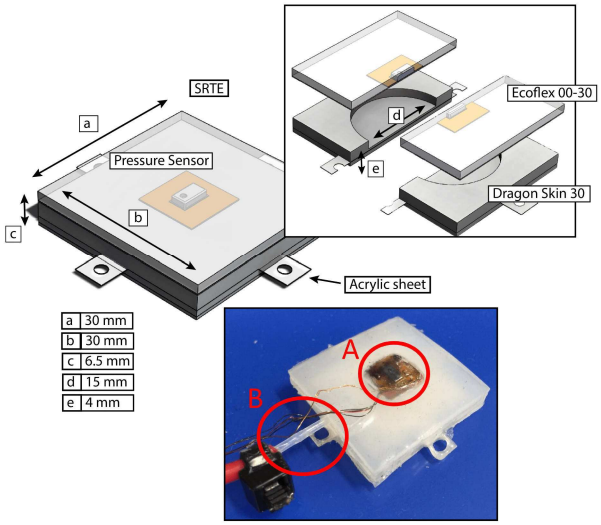

Fig. 3: A soft robotic tactile element (SRTE) in his isometric view (left). A) A barometric pressure sensor (MPL115A1) embedded in the membrane to obtain a tactile element. B) Tubing to fill the internal chamber with water causing expansion of the thin membrane.

different thickness (4 and 2.5mm, respectively. See Fig. 3). Therefore, the main effect of injecting an incompressible fluid in the hollow chamber is an expansion of the thin membrane facing the tissue, as represented in Fig. 4.

Under this assumption, we can define a linear relation between the volume V of the injected fluid and the vertical displacement δ of the membrane as $\delta = \Phi(V)$. This assumption should hold true even when the SRTE is pressing against a tissue, as long as the tissue offers a lower resistance to expansion (small indentations) than the remaining internal surface of the chamber. In case of very stiff tissue (large indentations), since the fluid is incompressible and we assume no pressure losses along the inlet line, the pressure reading would saturate even for small incremental volumes. For this reason, the sensor needs to be calibrated in the range of indentation required for the palpation task. For the prostate, as studied before, the maximum indentation would be 15% of the organ thickness [19].

Similar to [20], a barometric pressure sensor (MPL115A1, Freescale, USA) is embedded in the membrane to measure

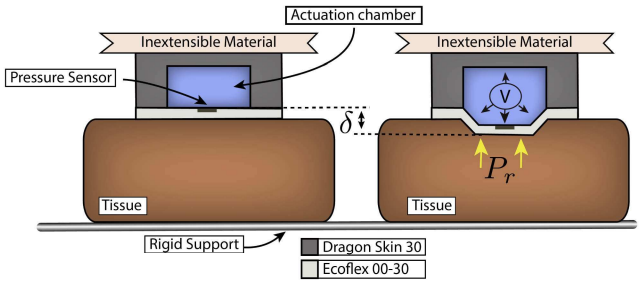

Fig. 4: The SRTE before (left) and after (right) injection of an incompressible fluid in the central chamber, highlighting the expansion of the wall facing the tissue.

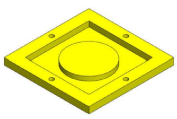

(a) Manufacturing starts with the cylindrical chamber mold.

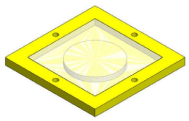

(b) Viscous silicone rubber is poured into the cylindrical chamber mold.

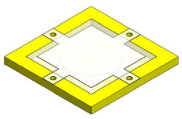

(c) Two layers of laser-cut, inextensible plastic sheet are positioned on top of the viscous silicone rubber.

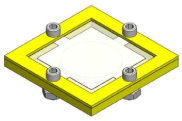

(d) A thin frame is positioned on the plastic sheet and tightly fit with screws.

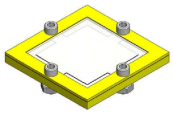

(e) Viscous silicone rubber is poured one more time and left to cure.

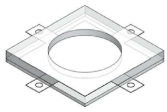

(f) After demolding, a disk shaped chamber is obtained.

(g) Sensor circuitry is made.

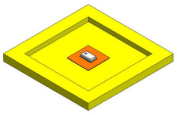

(h) Sensor is positioned inside a rectangular mold piece.

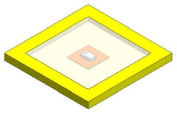

(i) Viscous silicone rubber is poured into the mold piece.

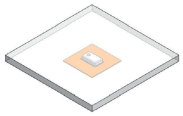

(j) Membrane is obtained once the silicone rubber is cured.

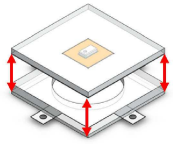

(k) The cylindrical chamber and the membrane are glued to each other using viscous silicone rubber.

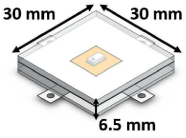

(l) Finished module is shown.

Fig. 5: Fabrication procedure for the SRTE.

the pressure P_r resisting the expansion of the chamber. For small indentation depths (i.e., less than one tenth of the organ thickness), it is reasonable to assume a linear elastic behaviour for the tissue [10]. A local tissue stiffness E can be estimated from a SRTE anchored on the target organ by injecting a known volume of incompressible fluid V and measuring the resulting pressure recorded by the sensor P_r as:

$$E \simeq P_r/\delta = P_r/\Phi(V). \tag{1}$$

B. SRTE Fabrication

Pressure sensing is realized by converting a barometric sensor into a tactile element [20]. Encapsulation of the transducer can be readily accomplished by suspending a circuit board with a mounted sensor in a mold and pouring in liquid silicone rubber precursor, which then cures to form the elastomer membrane. When molding is performed at atmospheric pressure, however, air is trapped within the sensor chip inside the ventilation hole. This results in low sensitivity because the surface pressure produces only small changes in the volume of the trapped air below the ventilation hole. A degassing procedure is hence required to address this issue. A 32 bits ARM micro-controller board (STM32F407, STMicroelectronics, Switzerland) and custom instruction libraries for handling communications with the sensor were used as the electronic interface. The step-by-step fabrication process is shown in Fig. 5 and its details are described below:

- Step-1: Silicone rubbers (Dragonskin 10) and (Ecoflex 00-30) were seperately poured in two different small containers and stirred well for a minute.
- Step-2: The mixture were degassed in a vacuum chamber following three cycles, in which the gauge pressure was gradually lowered to a value of approximately -76 kPa and kept constant for 10 minutes.

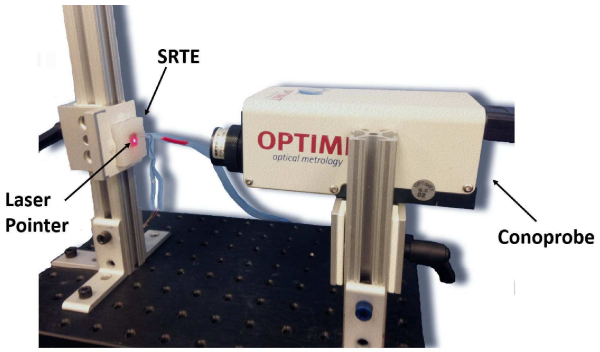

Fig. 6: A optical conoscopic holography sensor was used to measure deformation of the middle point of the SRTE membrane. The maximum deformation at different volumes is observed at the center of the SRTE.

- Step-3: The mixture was poured into separate molds for the cylindrical actuation chamber and the sensor membrane. Plastic molds were fabricated by rapid prototyping (Dimension SST 1200ES, Stratasys).
- Step-4: The molds were placed inside an oven at 60°C for 25 minutes.
- Step-5: Cured parts were taken out of the molds and bonded together using leftover uncured silicone rubber from Step-1. The bonded assembly was reheated inside the oven.
- Step-6: After bonding was achieved, a tubing was pierced through the wall inside the module until it reached the cylindrical hollow chamber.

III. Calibration

A. Volume-Displacement Characterization

Before assessing the overall functionality of the SRTE, a number of tests and characterization experiments were performed on test-bench. The first step was to verify the

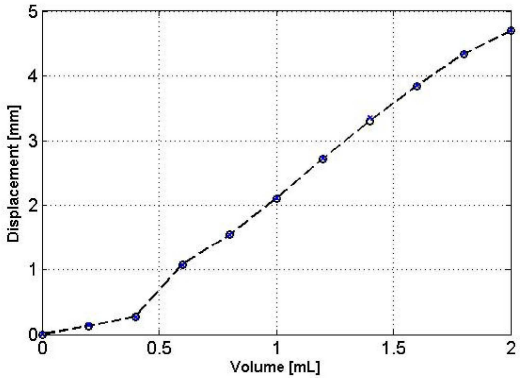

Fig. 7: Result of the Conoprobe measurement is shown above. A linear relationship between maximum deflection point and displacement can be made up to 2 mL. The x-axis represents the input volume and y-axis is the measured deflection in the membrane. Circles represent the collected data points.

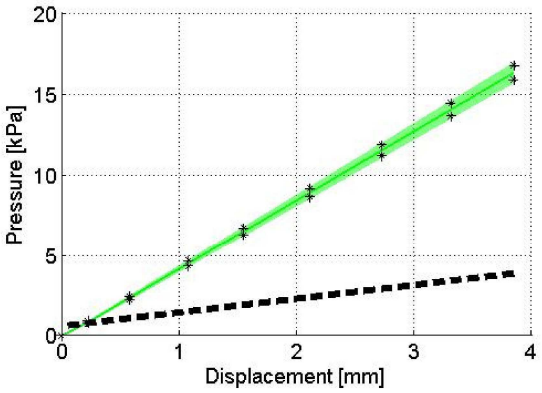

Fig. 8: Data acquired from the SRTE (black dashed line) was compared to the Instron output (Green) to obtain a calibration coefficient. Asterisks represent the variance of three sets of data points.

relationship between volume and vertical displacement when the tactile element is free to expand in air.

An optical conoscopic holography sensor (Conoprobe, Optimet, USA) was adopted as reference measurement system. The conoprobe laser was pointed at the upper circular surface of the SRTE, as shown in Fig. 6. The hollow chamber is expanded by injecting water in 0.2 mL increments from 0 to 2 mL. This test was repeated three times and error analysis was performed on the acquired data.

The average loading plot is represented in Fig. 7 with a standard deviation of ± 0.05 mm. The resulting data indicates that the relationship is linear for volumes from 0.6 to 2 mL that also correspond to the range of indentation required for tissue palpation [19].

B. Mechanical Stress Validation

In order to calibrate the SRTE, a tissue simulator was palpated with an Instron materials testing machine and three sets of trials were performed on the same tissue sample. Next, the same procedure was followed using the SRTE as the palpation device. The data from the two experiments were used to obtain a calibration coefficient for the SRTE. The tissue sample was fabricated by combining liquid plastic and hardener (PVC Regular Liquid Plastic and Regular Liquid Plastic Hardener, MF Manufacturing, USA 1:5 ratio). The sample was 40 mm thick with lateral sides of 100 mm.

The pressure data from the sensor was acquired using a custom designed test-bench. The test-bench consists of three aluminum bars interconnected together using L-brackets. The aluminum profiles were used to maintain the SRTE in contact with the tissue during the membrane's expansion. The same protocol adopted for the optical measurement was followed during each trial. The volume was increased with steps of 0.2 mL until 2 mL. In each step, the pressure reading from the sensor embedded in the SRTE was recorded. Measurements were interpolated using a polynomial curve to obtain a continuous relationship.

The same displacement was applied on the tissue sample using the Instron machine. The results of the two trials are plotted on Fig. 8. The sensor pressure data was compared with the reference data from the Instron. A non-dimensional calibration coefficient of 4.51 was obtained by overlying the two curves. The resulting pseudo-stiffness after calibration shows a maximum error of 3 kPa/mm with respect to the reference with a standard deviation of ± 0.5 kPa/mm.

IV. Suction Gripper Fabrication and Test

The suction grippers are fabricated by molding Dragonskin 30 and Ecoflex 00-30 (Smooth-On, PA, USA), using a 3D printed mold. Three grippers were fabricated with dimensions reported in Fig. 10. The same fabrication procedure as for the SRTE was followed: The silicone rubber was poured in a small container and stirred well, then the mixture is degassed and poured into the mold. The mold is spun at 3000 rpm along its vertical axis of symmetry. This procedure puts the silicone rubber in perfect contact with the internal surface, thus eliminating remaining imperfections (like air bubbles) due to the pouring process. Then, the molds are placed inside the oven at 60°C for 25 minutes. The resulting suction gripper is shown in Fig. 10

The grippers were attached at the end effector of a robotic manipulator (RV6SDL, Mitsubishi Corp., Japan) used as a materials testing machine (Fig. 10). A continuous vacuum pressure (-0.86 MPa) was applied for the adhesion of the bottom plate and the maximum force before detachment is measured. Results show that the DragonSkin 30 gripper is able to generate forces ranging from 1.2 to 1.4 N while the Ecoflex 00-30 provides forces roughly two-thirds of this force. The force achieved by the DragonSkin 30 suction gripper is twice the force needed for palpation, allowing the SRTE to maintain contact with the organ during operation.

V. Experimental Validation

The effectiveness in identifying buried structures inside tissue was first tested with a tissue phantom with buried lumps of a range of dimensions and depths (Fig. 11). Next, the same experiment was performed on a freshly excised chicken liver (approximately the dimension of a human prostate), to prove the feasibility of our approach on a

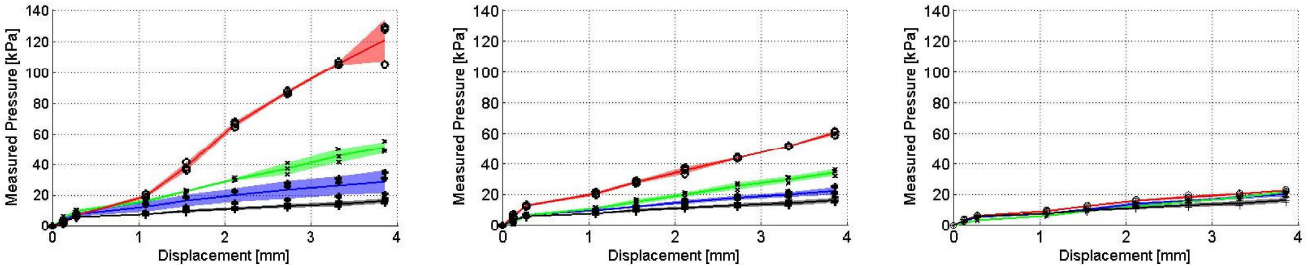

(a) Lumps at z_1. (b) Lumps at z_2. (c) Lumps at z_3.

Fig. 9: In each sub-figure different sized lumps at same depth are palpated. Markers designate data points. The solid curve is the mean of data points and the shaded region is the variance. Red, green, and blue colors represent tumor sizes big, medium, and small, respectively. The black color is the response of the healthy tissue.

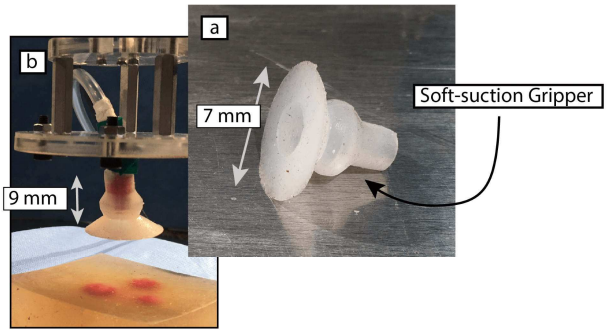

Fig. 10: a) Fabricated soft suction grippers. b) A suction gripper mounted on a custom material testing machine.

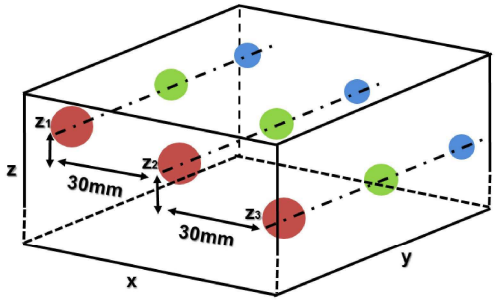

Fig. 11: Tissue simulator used for the experimental validation. Lump depths from the upper surfaces are 1.75mm, 3.25mm, and 4.75mm for z_1, z_2, and z_3. Each color represents a different diameter. Blue, green, and red circles correspond to lumps with 3mm, 6mm, and 9mm of diameters, respectively.

realistic round-shaped surface with irregular geometry, and also to understand the behaviour of our device on real tissue.

A. *Tissue Phantom Palpation Experiments*

The tissue phantom represented in Fig. 11 was constructed by combining different proportions of liquid plastics and hardener as explained in the previous section. Nine spherical lumps were made using rapid prototyping (material elastic modulus within 40-60 MPa). The dimension of the phantom and the lump locations, dimensions, and depths are shown in Fig. 11. The SRTE was placed manually above each buried lump with the pressure sensor facing the tissue. The same test-bench as in previous trials was used to maintain the SRTE in contact with the tissue. Water was injected into the cylindrical hollow cavity until it was full, but not deformed. Additional water was injected up to 1.6 mL in 0.2 mL increments to deform the SRTE surface that palpated the tissue phantom with the lumps.

Three sets of lumps were located at different depths z_1, z_2 and z_3, where z_3 represents the deepest lump set. At each set there were three different sized lumps at the same depth: r_1, r_2 and r_3, where r_3 is the largest lump.

Each lump was palpated three times to verify repeatability of the results. In our experiments we wanted to understand if the proposed SRTE was able to detect different sized lumps at the same depth. In the results we have gathered data on three plots in Fig. 9. In each plot, there are three different data-sets collected from different sized lumps at the same depth. The parameter that changes between the plots is the lump depth.

The results indicate that the SRTE was able to differentiate r_1, r_2 and r_3 sized lumps at z_1 and z_2 depths. However, it was not able to differentiate any sizes at the z_3 depth.

B. *Ex-vivo Chicken Liver Palpation Experiments*

A chicken liver was used for the *ex-vivo* trial. The liver had approximate lateral dimensions of 60 mm and a thickness of 15 mm, these dimensions are comparable to a human prostate. A wooden sphere was used to simulate a lump inside the tissue. An 8 mm piece was cut from a 25 mm sphere to achieve a flat bottom and avoid motion on a lab bench under the tissue. Instead of burying it inside the tissue, the cut-out piece was placed below the liver to simulate a tumor. This procedure resulted in an 8 mm lump at 15 mm depth, the full thickness of the liver. The anchoring mechanism was the same as in the tissue phantom trials. Again, water was used for palpating the tissue simulator with controlled volumetric increments and pressure response at each level was recorded.

The data obtained is presented in Fig. 12 and the tissue response was found to be similar to the simulated tissue phantom experiments. A qualitative change in mechanical stiffness can be observed when the liver is palpated with

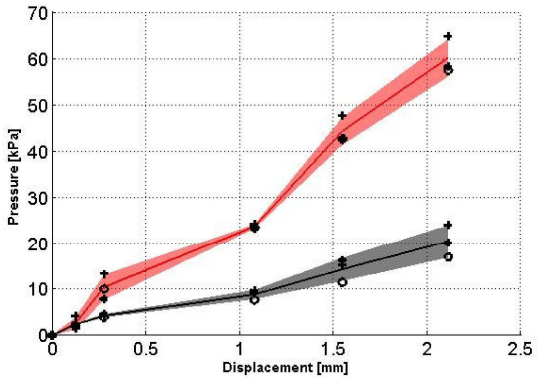

Fig. 12: The shaded region represent mean and variance of three sets of data points obtained from *ex-vivo* trial. The black color represent the healthy tissue and the red color represents the tissue above the buried lump. The x-axis represents the maximum deformed point on the SRTE membrane in mm. The y-axis is the measured pressure from the sensor at different deformations.

and without the wooden lump.

VI. CONCLUSIONS AND FUTURE WORK

This work demonstrates the capability of a soft robotic tactile element (SRTE) as a palpation module to qualitatively detect tumors buried inside tissue. To confirm this idea, tests on a tissue phantom and a chicken liver were conducted. A characterization of the barometric pressure sensor data was made in comparison with the pressure values obtained from an Instron material testing machine. A non-dimensional calibration coefficient of 4.51 was computed between the RSTE and the reference pressures.

To demonstrate the performance of the SRTE, a custom tissue phantom with different-size lumps buried at three different depths was used. The SRTE was able to differentiate between 3 mm, 6 mm, and 9 mm diameter lumps buried at 1.75 mm and 3.25 mm. A qualitative difference in local stiffness values of the tissue was not observed for lumps at 4.75 mm depth. This result is promising considering that the maximum indentation depth was 4 mm. A similar test was performed using a freshly excised chicken liver with a lump embedded about 15 mm below the tissue surface and the SRTE was able to clearly identify the region with the lump from the surroundings.

Suction grippers were shown to be the most promising solution for gripping to the organ. During the trial, they were able to compensate roughly twice the maximum expansion forces exerted on the tissue allowing for a stable interface with the tissue during palpation. Future works include test and control of a SRTE matrix on a curved tissue surface with the aim of quantitatively estimating the position of embedded lumps within the organ.

ACKNOWLEDGMENT

This work was supported by the National Science Foundation under grant no. IIS-1453129. Any opinions, findings and conclusions, or recommendations expressed in this material are those of the authors and do not necessarily reflect the views of the National Science Foundation.

REFERENCES

[1] P. Puangmali, H. Liu, L.D. Seneviratne, P. Dasgupta, and K. Althoefer. Miniature 3-axis distal force sensor for minimally invasive surgical palpation. *IEEE/ASME Transactions on Mechatronics*, 17(4):646–656, 2012.

[2] National Cancer Institute: `www.cancer.gov`.

[3] K.T. Nguyen, T.C. Gamblin, and D.A. Geller. World review of laparoscopic liver resection. *Annals of Surgery*, 250(5):831–841, 2009.

[4] J. Finkelstein, E. Eckersberger, H. Sadri, S.S. Taneja, H. Lepor, and B. Djavan. Open versus laparoscopic versus robot-assisted laparoscopic prostatectomy: the European and US experience. *Reviews in Urology*, 12(1):35, 2010.

[5] P. Dario and M. Bergamasco. An advanced robot system for automated diagnostic tasks through palpation. *IEEE Transactions on Biomedical Engineering*, 35(2):118–126, 1988.

[6] R.D. Howe, W.J. Peine, D.A. Kantarinis, and J.S. Son. Remote palpation technology. *IEEE Engineering in Medicine and Biology Magazie*, 14(3):318–323, 1995.

[7] S. Schostek, M.J. Binser, F. Rieber, C.N. Ho, M.O. Schurr, and G.F. Buess. Artificial tactile feedback can significantly improve tissue examination through remote palpation. *Surgical Endoscopy*, 24(9):2299–2307, 2010.

[8] M.P. Ottensmeyer and J.K. Salisbury Jr. *In Vivo Data Acquisition Instrument for Solid Organ Mechanical Property Measurement*, volume 2208. 2001.

[9] F.L. Hammond, R.K. Kramer, Q. Wan, R.D. Howe, and R.J. Wood. Soft tactile sensor arrays for micromanipulation. In *Intelligent Robots and Systems (IROS), 2012 IEEE/RSJ International Conference on*, pages 25–32, Oct 2012.

[10] H. Liu, J. Li, X. Song, L.D. Seneviratne, and K. Althoefer. Rolling indentation probe for tissue abnormality identification during minimally invasive surgery. *IEEE Transactions on Robotics*, 27(3):450–460, 2011.

[11] G.L. McCreery, A.L. Trejos, M.D. Naish, R.V. Patel, and R.A. Malthaner. Feasibility of locating tumours in lung via kinaesthetic feedback. *The International Journal of Medical Robotics and Computer Assisted Surgery*, 4(1):58–68, 2008.

[12] A. Talasaz and R.V. Patel. Integration of force reflection with tactile sensing for minimally invasive robotics-assisted tumor localization. *IEEE Transactions on Haptics*, 6(2):217–228, 2013.

[13] M.T. Perri, A.L. Trejos, M.D. Naish, R.V. Patel, and R.A. Malthaner. New tactile sensing system for minimally invasive surgical tumour localization. *The International Journal of Medical Robotics and Computer Assisted Surgery*, 6(2):211–220, 2010.

[14] J.C. Gwilliam, Z. Pezzementi, E. Jantho, A.M. Okamura, and S. Hsiao. Human vs. robotic tactile sensing: Detecting lumps in soft tissue. In *IEEE Haptics Symposium*, pages 21–28, 2010.

[15] S. McKinley, A. Garg, S. Sen, R. Kapadia, A. Murali, K. Nichols, S. Lim, S. Patil, P. Abbeel, A.M. Okamura, and K. Goldberg. A disposable haptic palpation probe for locating subcutaneous blood vessels in robot-assisted minimally invasive surgery. In *IEEE International Conference on Automation Science and Engineering*, pages 1151–1158, 2015.

[16] R. E. Goldman, A. Bajo, and N. Simaan. Algorithms for autonomous exploration and estimation in compliant environments. *Robotica*, 31(1):71–87, 2013.

[17] O.C. Jeong and S. Konishi. The self-generated peristaltic motion of cascaded pneumatic actuators for micro pumps. *Journal of Micromechanics and Microengineering*, 18(8):085017, 2008.

[18] D. Vonck, R. H. M. Goossens, D. J. van Eijk, I. H. J. T. de Hingh, and J. J. Jakimowicz. Vacuum grasping as a manipulation technique for minimally invasive surgery. *Surgical Endoscopy*, 24(10):2418–2423, 2010.

[19] M. Beccani, C. Di Natali, M. E. Rentschler, and P. Valdastri. Wireless tissue palpation: Proof of concept for a single degree of freedom. In *Robotics and Automation (ICRA), 2013 IEEE International Conference on*, pages 703–709, 2013.

[20] Y. Tenzer, L.P. Jentoft, and R.D. Howe. The Feel of MEMS Barometers: Inexpensive and Easily Customized Tactile Array Sensors. *Robotics Automation Magazine, IEEE*, 21(3):89 – 95, 2014.